A Thin Film Wireless Passive Multiplexed Wearable Biomarker Sensor

Ruitong Chen
Alfred E. Mann Department of Biomedical Engineering
University of Southern California
Los Angeles, CA, USA
ruitongc@usc.edu

Ellis Meng
Alfred E. Mann Department of Biomedical Engineering
University of Southern California
Los Angeles, CA, USA
ellis.meng@usc.edu

***Abstract*—Electrochemical sensor-integrated wearable devices can noninvasively monitor biomarkers present in sweat and interstitial fluid to provide insights on physiological health status. Current approaches often require rigid electrical components for signal processing and data transmission, which can negatively impact wearability. Passive sensing formats to eliminate rigid, discrete electronics have been explored but are largely limited to single marker detection. We investigate an alternative passive multiplexed sensing paradigm in which an entire system can be constructed in a thin, flexible film using polymer microfabrication techniques. Cortisol and sodium were selected as model molecules for the purpose of demonstrating wireless biomarker measurement using this system based on the principle of reflected impedance. Presence of each triggers changes in different circuit components of the secondary side equivalent, further demonstrating that sensing via different modes is possible using this a proof-of-concept multiplexed biomarker sensor constructed entirely on a flexible and biocompatible thin film.**

Keywords—Electrochemical sensors, multiplexed sensing, wireless sensing, passive sensing, wearable device

I. Introduction

Wearable devices have garnered increased interest as a format for non-invasive monitoring of analytes in sweat or interstitial fluid. Most approaches involve the integration of sensors on a flexible substrate with rigid, off-the-shelf electronic components for signal processing and data transmission which limit achievable device profile and wearability [1], [2]. Passive sensing mechanisms, which eliminate the need for discrete electronics, have been reported but are often limited to single marker detection.

We previously introduced a new concept for wireless and passive transduction of electrochemical impedance using reflected impedance and is accomplished without integrated circuits or discrete electrical components [3]. Briefly, the sensing modality utilizes the inductive coupling present between a primary and secondary coil. As the load on the secondary coil changes, the impedance readout of the primary coil is also affected, therefore achieving passive transduction through interrogating primary coil impedance. A prototype 16-turn microfabricated thin coil terminating in square electrodes was used to demonstrate the concept but suffered from low sensitivity, largely stemming from the suboptimal sensor layout. An improved layout was explored which used a bridge capacitor to simplify fabrication and a pair of interdigitated electrodes (IDEs) for the sensing interface [4]. The IDE format increased sensing surface area which in turn lowered the baseline and increased sensitivity. Since two distinct metal layers are required to form the IDEs, a bridge capacitor provided a convenient alternative to using a via while also providing a means to tune coil resonance and overall performance. Three distinct electrochemical biomarker sensing modes (enzymatic sensing, immunosensing, and aptasensing) were realized and demonstrated by using different functional coatings on the IDEs.

Here, we expand on our original concept and report a novel, compact multiplexed sensing system suitable for wearable applications. The system consists of a single primary coil for readout and two nested microfabricated secondary coils attached to sensing IDEs (Fig. 1A). The device is embedded in a thin, flexible film that conforms well to the human skin (Fig. 1B).

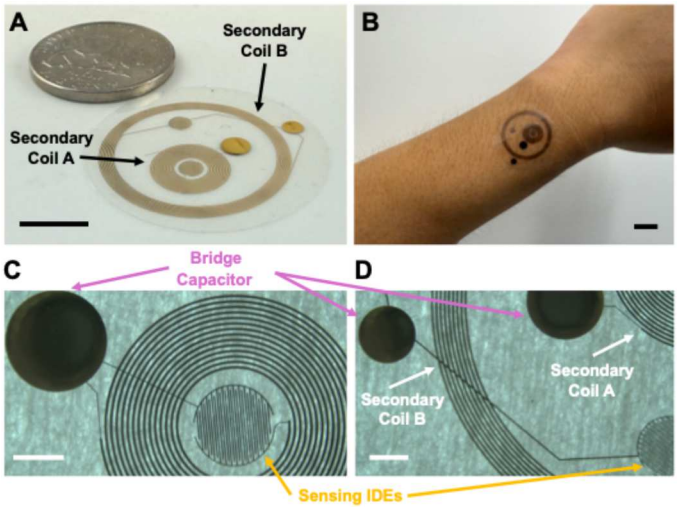

Fig. 1. (A) Optical image of device compared to a U.S. quarter. Scale bar = 1 cm. (B) Optical image of flexible device conforming to arm of volunteer. Scale bar = 1 cm. (C) Closeup image showing details of secondary coil A. Scale bar = 2 mm. (D) Closeup image showing details of both secondary coil A and B. Scale bar = 2 mm.

This work was supported in part by the National Science Foundation (NSF) under Award ECCS-1933318. Ellis Meng (ellis.meng@usc.edu) is the corresponding author.

The two secondary coil geometries (A & B) were designed to resonate at different frequencies and provide sensing selectivity (Fig. 1C and 1D). Each coil included an dedicated IDE pair for sensing that was treated using a different surface modification technique. Device A's IDE surface was modified to be sodium selective using an ion selective membrane whereas Device B's IDE surface targeted cortisol via an aptamer. To minimize footprint of the readout system and achieve matching resonant frequencies between the primary coil and the secondary coil for optimized sensitivity, a tuning circuit was utilized to achieve two resonant frequencies while using only single primary coil. The sensing system was first characterized then multiplexed detection of two biomarkers was demonstrated.

II. Methods

A. Device Fabrication

The sensing system was fabricated using standard Parylene C microfabrication techniques [5]. Briefly, a 10-micron thick Parylene C layer was deposited onto a 4-inch silicon wafer via chemical vapor deposition (CVD). Two metal layers (10 nm Ti/ 300 nm Au deposited via e-beam both at 2 Å/s), separated by a 4-micron thick Parylene C layer, were photolithographically-patterned to realize the coil, bridge capacitor, and IDEs. A 10-micron thick Parylene C passivation layer covered the majority of the device except for the IDEs which were exposed using a deep reactive ion etcher.

B. Testing Setup

The testing setup to characterize the sensing system is summarized in Fig. 2A. An LCR meter and a custom-built LabVIEW user interface was used to sweep frequency across the targeted range and record the impedance response. A commercially available wireless power transfer coil was used as the primary coil (Fig. 2B). A tuning circuit consisting of an 19 µH inductor was used to tune the primary coil resonant frequency when needed.

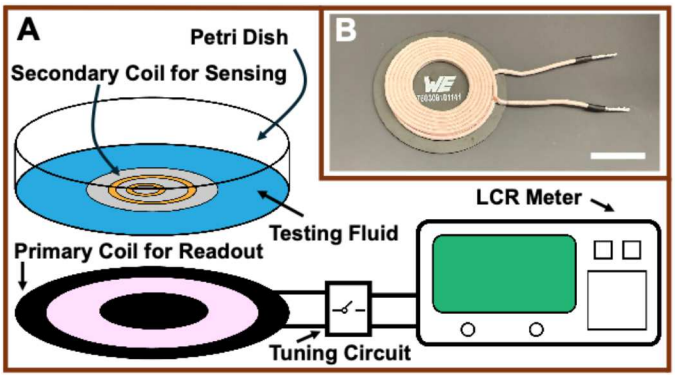

Fig. 2. (A) Illustration depicting testing setup. (B) Optical image showing wireless power transfer coil used for primary coil readout. Scale = 1 cm.

C. Multiplexed Sensing Theory

The working principle of passive electrochemical biomarker sensing was adopted from our prior work [4]. Each secondary coil has a gold IDE with the surface modified to be selective to a biomarker, either cortisol or sodium. As the biomarker concentration changes in the vicinity of the sensor, the associated sensor response can be quantified by interrogating the primary coil's impedance response. Cortisol sensing is likely a faradaic process. The unbound end of the aptamer is modified with methylene blue, a common redox probe. When aptamer binds to cortisol, methylene blue moves closer to the electrode surface and induces a detectable charge transfer resistance change [6]. Ion sensing relies on the selectivity provided by the ion selective membrane and does not rely on the electroactive properties of gold sensor surface. Multiple circuit elements (solution resistance, ion selective membrane capacitance, and membrane coating related constant phase element) may contribute to the response, depending on variables such as the testing frequencies and ion concentrations [7].

Multiplexed sensing sensitivity and selectivity stems from the difference in resonant frequencies between the two coils as well as the inherently different electrochemical sensing modes. When the tuning circuit is disconnected, the primary coil resonates with secondary coil B and therefore is sensitive to cortisol level changes (Fig. 3A). When the tuning circuit is connected, the primary coil resonant frequency shifts and now resonates with secondary coil A, which is sensitive to sodium level changes (Fig. 3B).

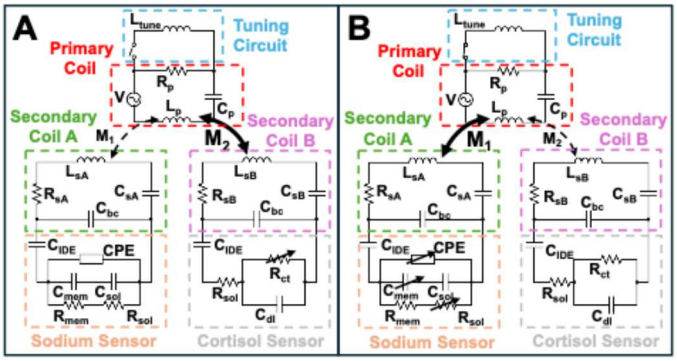

Fig. 3. Equivalent circuit model for the primary and secondary circuits. (A) The tuning circuit is disconnected and the primary coil resonates with secondary coil B. Changes in cortisol level induces detectable changes in charge transfer resistance. (B) The tuning circuit is connected and the primary coil resonantes with secondary coil A. Changes in sodium level induces various circuit component changes and that can be detected by the primary coil reader.

D. Sensing System Characterization

The individual coil/sensor pairs (A & B) were characterized prior to surface modification. First, the influence of alignment accuracy with the primary coil was investigated. Each secondary coil was centered and sensitivity evaluated using protocols introduced previously [4]. Briefly, sensors were exposed to varying solution conductivities from 0 to 160 mS/cm. Vertical separation distance was characterized by stacking 1 mm thick glass slides between the primary and secondary while using 1× PBS as the test fluid. Both impedance magnitude at resonance and resonant frequency were recorded and used for evaluation in all characterization studies.

E. Sensor Surface Modification Protocol

IDE surfaces were first cleaned using Nanostrip for five minutes. Cortisol aptamer functionalization process took place in a dark at room temperature while sodium selective membrane modification was performed in ambient environment.

Cortisol targeting aptamer was immobilized on the sensor surface [6]. Briefly, 100 µM of aptamer solution was first incubated with excess tris(2-carboxyethyl) phosphine (TCEP) for 1 hour followed by dilution into 500 nM in 1× phosphate-buffered saline. The sensor was incubated in the aptamer solution for one hour followed by overnight incubation in 10 mM 6-mercapto-1-hexanol (MCH) solution.

A sodium ion selective membrane process was adopted from previous work [8]. Since gold does not provide robust ion-to-electron transduction, single walled carbon nanotubes (SWCNTs) were selected for its well-controlled structures and tunable surfaces [9]. SWCNT ink was first drop casted onto the sensor surface and baked at 50 °C for one hour to evaporate solvents, followed by drop casting sodium selective sensing membrane onto the SWCNT surface and drying overnight to provide sufficient bonding between the two drop casted layers. Finally, the sensor was conditioned in 300 mM NaCl solution for thirty minutes to facilitate sufficient ion exchange.

F. Biomarker Sensing

A calibration curve for each sensor was first established in varying concentrations of target molecule at physiological relevant ranges in 1× PBS. The thin-film device was held in a petri dish and positioned above the primary coil based on alignment characterization results. Multiplexed sensing was demonstrated and responses of both coils were recorded at 2-minute intervals. At the beginning, 175 mM sodium and 750 mM cortisol in 1× PBS were introduced into the system. Next, sodium concentration was lowered to 125 mM while holding cortisol at 750 mM. Finally, cortisol concentration was reduced to 250 mM while keeping sodium at 125 mM.

III. Results

The impedance spectra of the primary coil revealed a 12.3 MHz resonant frequency (Fig. 4A). After connecting to the tuning circuit, the resonant frequency recorded was 15.5 MHz (Fig. 4B), demonstrating the feasibility of using a tuning circuit to achieve two resonant frequencies with a single primary coil.

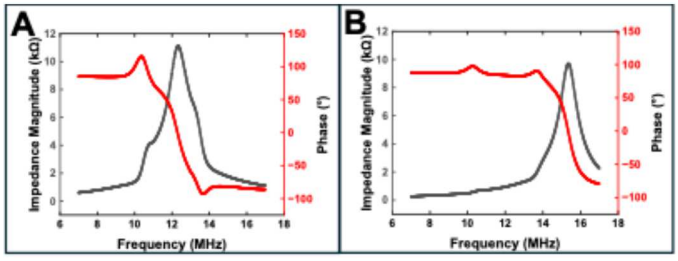

Fig. 4. Impedance spectra of primary coil when the tuning circuit was (A) disconnected and (B) connected.

Secondary coil misalignment with the primary coil changed the coupling coefficient and therefore affected sensitivity. The two secondary coils in the system have offset centers, resulting in a 2 mm misalignment between the aligned and unaligned coils. As shown in Fig. 5A and 5B, secondary coil A sensor sensitivity was significantly decreased with misalignment where coil B sensor was mostly unaffected (Fig. 5C and 5D). Therefore, subsequent experiments involving both coils used the strategy of only aligning the primary to secondary coil A.

As the distance between the primary and the secondary coils increased, the inductive coupling strength changed, negatively impacting sensitivity. Both secondary coil A and B sensors exhibited a similar trend as both impedance magnitude as well as resonant frequency increased in response to increasing separation distance (Fig. 6A and 6B). As expected, a decrease in sensitivity was observed in both coils, where the sensor for coil A became nearly unresponsive at 10 mm separation distance (Fig. 6B and 6C) and coil B's sensor sensitivity reduced by more than half at the same separation distance (Fig. 6E and 6F).

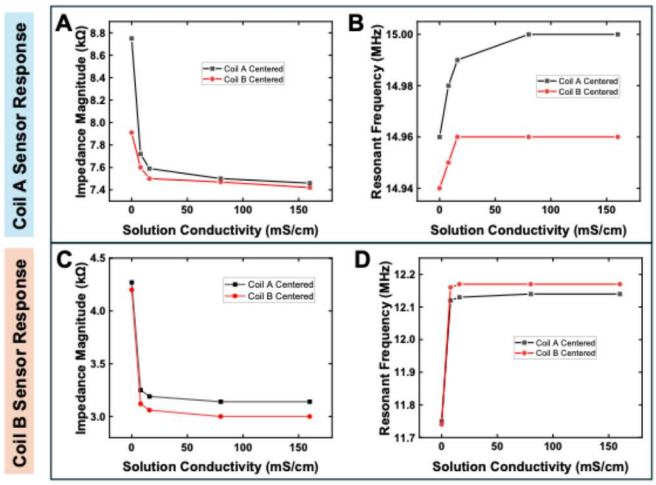

Fig. 5. Secondary coil A sensor impedance magnitude response (A), (B) resonant frequency response and coil B impedance magnitude response (C), (D) resonant frequency response at two alignment schematics.

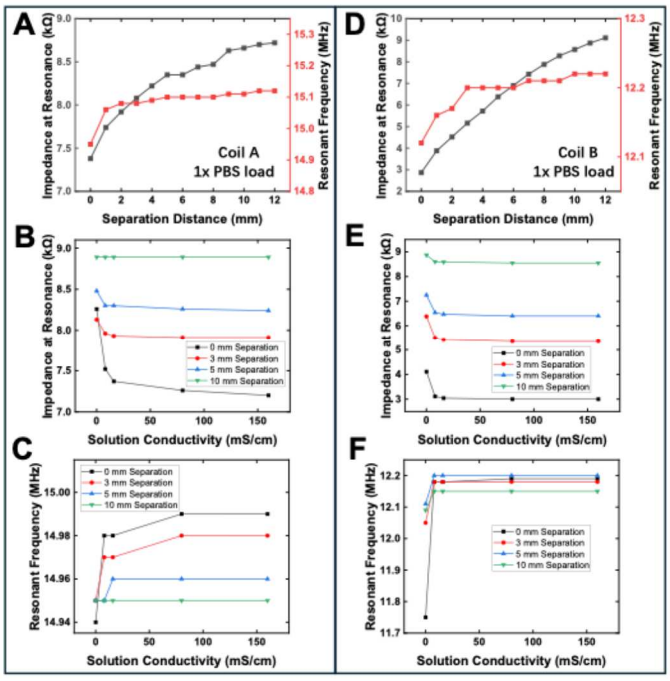

Fig. 6. Response to coil separation for secondary coil (A) A and (D) B sensors. Impedance magnitude response to varying solution conductivies over 0 to 10 mm of separation for secondary coil (B) A and (E) B sensors. Resonant frequency response to varying solution conductivies over 0 to 10 mm of separation for secondary coil (C) A and (F) B sensors.

Sensor surfaces were modified with respective biomarker recognition elements and a calibration curve was constructed. As shown in Fig. 7A, both the impedance magnitude and resonant frequency for the secondary coil B sensor exhibited a linear response to cortisol concentration. On the other hand, only the impedance magnitude response for secondary coil A sensor was linearly correlated to sodium concentration; resonant frequency response was nonlinear (Fig. 7B). As such, only impedance magnitude response was monitored for multiplexed sensing experiments.

The secondary coil B sensor exhibited excellent sensitivity and selectivity during multiplexed testing, where the impedance magnitude increased with a decrease in cortisol concentration, a trend matching its calibration curve. There was no change in response when sodium concentration varied (Fig. 7C). On the other hand, the secondary coil A sensor exhibited poor selectivity; impedance response increased with decreasing sodium concentration but also increased in response to decreasing cortisol concentration (Fig. 7D).

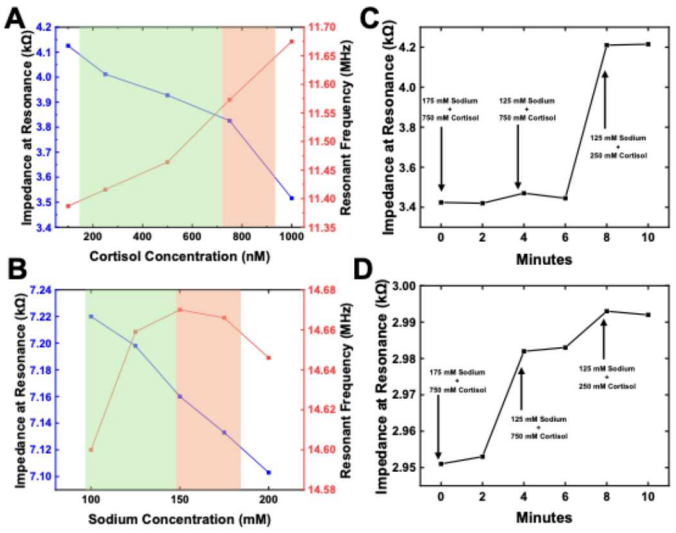

Fig. 7. (A) Secondary coil B sensor response to varying cortisol concentration. (B) Secondary coil A sensor response to varying sodium concentration. The green highlighted region indicates normal physiolgical levels and red indicates an abnormal elevated level. (C) Secondary coil B sensor response during multiplexed sensing. (D) Secondary coil A response during multiplexed study.

IV. Discussion and Conclusion

In this work, we demonstrate the potential of a wireless, passive multiplexed wearable biomarker sensing system consisting only of a thin film, providing an alternative to conventional approaches that use active electronics integrated with sensors onto a flexible substrate. The thin film format may be preferred in applications where a low profile, conforming device is required.

Both cortisol and sodium sensing were demonstrated and while the selectivity needs to be improved for the secondary coil A, this is likely achievable by addressing parasitic coupling between coil B and the primary coil at the frequency where only coil A should produce measurable responses. This is being investigated in ongoing work.

Also, biomarkers were only tested in a simple biofluid model (1× PBS) which is sufficient to demonstrate the concept. Future studies will require evaluation in more realistic test fluids such as artificial serum, interstitial fluid, or sweat. This will allow further evaluation of interfering species as well as development of new surface functionalization strategies to incorporate detection of other biomarkers .

Acknowledgment

The authors thank Nikolas Barrera for discussion on coil geometry design and Farbod Amirghasemi for discussion on sensor surface modification processes. All authors thank staff members of the O'Brien Nanofabrication Laboratory at the University of Southern California.

References

[1] M. Bariya, H. Y. Y. Nyein, and A. Javey, "Wearable sweat sensors," *Nat Electron*, vol. 1, no. 3, pp. 160–171, Mar. 2018, doi: 10.1038/s41928-018-0043-y.

[2] E. Ramirez *et al.*, "A Wearable System for Wireless and Multiplexed Molecular Sensing Via Solid Microneedles," in *2025 IEEE 38th International Conference on Micro Electro Mechanical Systems (MEMS)*, Kaohsiung, Taiwan: IEEE, Jan. 2025, pp. 383–386. doi: 10.1109/MEMS61431.2025.10918177.

[3] A. Baldwin, L. Yu, M. Pratt, K. Scholten, and E. Meng, "Passive, wireless transduction of electrochemical impedance across thin-film microfabricated coils using reflected impedance," *Biomed Microdevices*, vol. 19, no. 4, p. 87, Dec. 2017, doi: 10.1007/s10544-017-0226-8.

[4] R. Chen, A. Baldwin, E. Ramirez, and E. Meng, "A Thin Film Coil with Integrated Electrochemical Sensor for Wireless and Passive Biomarker Sensing," in *2025 IEEE 38th International Conference on Micro Electro Mechanical Systems (MEMS)*, Kaohsiung, Taiwan: IEEE, Jan. 2025, pp. 327–330. doi: 10.1109/MEMS61431.2025.10917430.

[5] B. J. Kim and E. Meng, "Micromachining of Parylene C for bioMEMS: Micromachining of Parylene C for BioMEMS," *Polym. Adv. Technol.*, vol. 27, no. 5, pp. 564–576, May 2016, doi: 10.1002/pat.3729.

[6] C. Larson, K. Plaxco, and E. Meng, "Materials Characterization for Microneedle-Based Molecular Sensing Platform," in *2024 IEEE 37th International Conference on Micro Electro Mechanical Systems (MEMS)*, Austin, TX, USA: IEEE, Jan. 2024, pp. 352–355. doi: 10.1109/MEMS58180.2024.10439524.

[7] E.-M. Korek, R. Teotia, D. Herbig, and R. Brederlow, "Electrochemical Impedance Spectroscopy for Ion Sensors with Interdigitated Electrodes: Capacitance Calculations, Equivalent Circuit Models and Design Optimizations," *Biosensors*, vol. 14, no. 5, p. 241, May 2024, doi: 10.3390/bios14050241.

[8] F. Amirghasemi *et al.*, "LiFT (a Lithium Fiber-Based Test): An At-Home Companion Diagnostics for a Safer Lithium Therapy in Bipolar Disorder," *Adv Healthcare Materials*, vol. 13, no. 18, p. 2304122, Jul. 2024, doi: 10.1002/adhm.202304122.

[9] R. Chen, F. Amirghasemi, H. Ma, V. Ong, A. Tran, and M. P. S. Mousavi, "Toward Personalized Treatment of Depression: An Affordable Citalopram Test based on a Solid-Contact Potentiometric Electrode for at-Home Monitoring of the Antidepressant Dosage," *ACS Sens.*, vol. 8, no. 10, pp. 3943–3951, Oct. 2023, doi: 10.1021/acssensors.3c01545.